THE JOURNAL OF PHYSICAL CHEMISTRY A

Article

pubs.acs.org/JPCA

Role of Capping Agent in Wet Synthesis of Nanoparticles

Chi M. Phan*[,†] and Hoang M. Nguyen[†,‡]

[†]Nanochemistry Research Institute and Department of Chemical Engineering, Curtin University, GPO Box U1987, Perth, Western Australia 6845, Australia

[‡]The University of Da Nang—University of Science and Technology, Da Nang 59000, Vietnam

ABSTRACT: Aqueous-based synthesis is one of the most popular methods to prepare nanoparticles. In these procedures, surfactants are needed to regulate the growth and final particle size. While there are numerous evidence on the decisive role of surfactants, a quantitative description remains elusive. This study develops a theoretical model to correlate the surfactant activities to particle growth. In the model, the "penetrability" of ions within surfactant layer is used to combine surface reaction and adsorption/desorption processes. The penetrability was then directly correlated to surfactant size. The theory was verified by synthesis of iron oxide nanoparticles with series of cationic surfactants. Eight surfactants, with same headgroup and increasing hydrocarbon tail, were employed. The experimental data showed a deterministic correlation between surfactant tails and particle size. The experimental correlation between surfactant length and particle size was predicted by the model. The modeling results verify the role of surfactant as capping agent during particle growth. More importantly, it provides a theoretical framework to control particle size in wet synthesis.

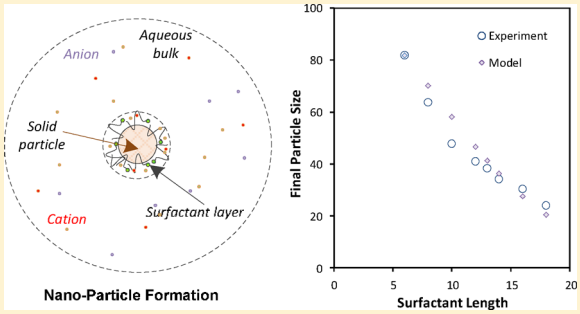

1. INTRODUCTION

Size control of nanoparticles remains a critical process for successful application of nanotechnology. In recent years, the synthesis nanoparticle from solution technique has been widely applied for synthesizing nanoparticle of a wide range of material.[1,2] The small size in these materials confers new properties and opens up possibilities of novel applications.[3,4] The aqueous colloidal synthetic approach[5] remains an attractive pathway for aqueous synthesis due to its simplicity and affordability. In these processes, a surfactant is critically needed as a capping agent.[6] Without the surfactants, the metal oxides would form a continuous phase instead of discrete nanoparticles. In colloid science, it is well-accepted that the surfactants prevent particle aggregation, due to surfactant adsorption layer on the particles surface. The selective adsorption of surfactant has been manipulated to control the growth direction, thus particles shape[7] to nonspherical forms, such as disk or rod. These evidence verify that the surfactant layer formed during particle growth and can regulate the reaction kinetics. Yet, the role of surfactants on particle growth remains unquantified.

A proper understanding on the role of surfactants can open up a possibility to control particle size by varying surfactant. At molecular level, the role can be manipulated by a simple variation in size/structure of the surfactant. In the literature, numerous studies have shown that surfactant size can control micelle shape and size,[8,9] which serve as a template for particle nucleation.[10] More importantly, experimental results[10] have demonstrated the influence of surfactants on the size of metal oxide particles. Our previous studies, in which the size of surfactants was varied systematically, have verified a deterministic role of surfactant length on particles size of both iron[1] and tungsten oxides.[11] However, a quantitative correlation between nanoparticle size and surfactant size is not available.

This study aims to develop and verify a theoretical correlation between surfactant structure and final particle size. A theoretical framework is developed to incorporate the presence of surfactant molecules into particle formation process. The model is then applied to experimental data of iron-oxide nanoparticles, which were prepared with a series of cationic surfactants. Eight cationic surfactants, with increasing size, were systematically selected. The experimental results are used to verify the model. Ultimately, the verified correlation between surfactant size and final particle size provides a new pathway to control particle size in sol—gel method.

2. THEORETICAL DEVELOPMENT

In general, particle formation in solution-based synthesis involves two processes: nucleation and growth. Surfactants, which can be termed as "capping agent" in the procedure, can influence both processes. Surfactant micelles can form a template for nucleation. The influence of surfactant length on the micelles size has been quantitatively verified.[9] Hence, surfactant length can influence critical nuclei size, which can be predicted by the classical nucleation theory.[12] However, typical micelle radius is less than 0.3 nm,[13] but the typical metal oxide particles are in order of 10 nm. As results, the particle growth is the decisive step and is the main focus of this study.

Received: March 7, 2017
Revised: April 10, 2017
Published: April 11, 2017

DOI: 10.1021/acs.jpca.7b02186
J. Phys. Chem. A 2017, 121, 3213−3219

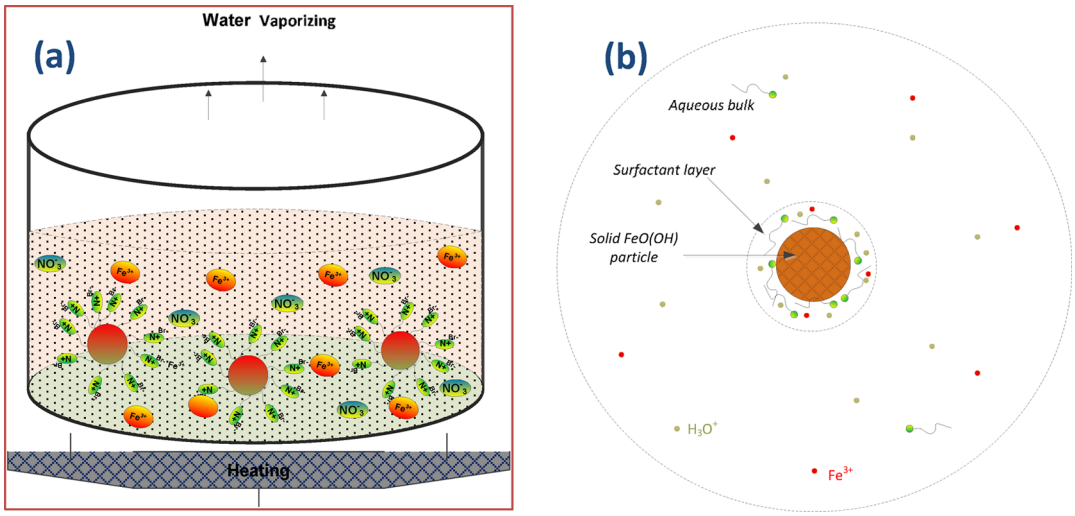

Figure 1. (a) Schematic representation of sol synthesis process of iron oxide. (b) Surfactant layer during FeO(OH) particle growth (anions are not included for clarity).

The particle growth in aqueous solution is governed by two elementary processes: diffusion from bulk to particle surface and binding reaction between ions and solid particle.[14] Depending on the physical conditions, either diffusion or surface reaction can be a rate-controlling process.[15] The theory on diffusion-controlled growth has been proposed more than six decades ago.[16] Yet the model does not account for either the reaction rate or the role of a capping agent. The modeling of reaction process, in contrast, is not well-developed. A general framework has been proposed to include both diffusion and surface reaction.[17] Nevertheless, the model cannot be solved analytically. Furthermore, the role of surfactant has not been incorporated into the model. As reviewed by Rempel and coauthors,[17] the available theoretical frameworks cannot predict the final particle size from the reaction-limited process. In contrast, the capping agent directly influences the rate of the surface reaction. Consequently, a new model is required to quantify the role of surfactant into the surface reaction.

2.1. Particle Growth. The formation of iron oxide, which is an important nanomaterial,[11] is selected for theoretical model in this study. The reaction pathway for Fe_2O_3 is well-established (Figure 1a). In this process, the typical reagents are Fe^{3+} salts (with either Cl^- or NO_3^-),[6] which can be hydrolyzed to form suspended colloids of FeO(OH). The overall hydrolysis/condensation is given by[18]

$$Fe^{+3} + 5H_2O \leftrightarrow FeO(OH) + 3H_3O^+ \quad (1)$$

Upon further heating, FeO(OH) particles are transformed to stable phase of iron oxide:

$$2FeO(OH) \leftrightarrow Fe_2O_3 + H_2O \quad (2)$$

The particle size of Fe_2O_3 is directly proportional to the size of FeO(OH), which is regulated during the "sol" formation process. The typical capping agent for iron oxide is a cationic surfactant, such as alkyl trimethylammonium bromide, or $C_nH_{2n+2}(CH_3)_3NBr$. As the surfactant molecules (Figure 1b) cover the particle surface, the surfactant layer controls the mass transfer and regulates the reaction rate on surface.

In this model, the surfactant layer on particle surface assumingly acts as a barrier for ions transfer. The layer is partially penetrable by ions in the system. The degree of penetrability depends on the nature of the surfactant and is a main parameter in the model. Since the penetration is limited, the surface reaction is the rate-setting process in the overall particle growth. The overall mass transfer of ions through surfactant zone involves two simultaneous steps: (i) adsorption/desorption between the bulk and surfactant zone; and (ii) binding reaction from surfactant zone to the solid surface. Hence, an overall mathematical model is developed to describe these two steps before predicting the overall mass transfer.

During the particle growth, growth rate of the particles equals to the flux of Fe^{3+} in binding reaction:[16]

$$Q = \frac{\rho}{M}\frac{d}{dt}\left(\frac{4}{3}\pi {R_p}^3\right) = \frac{\rho}{M}4\pi {R_p}^2\frac{dR_p}{dt} \quad (3)$$

where Q (mol/s) is the flux of Fe^{3+}, ρ is the partial density of Fe in solid (Fe in FeO(OH)), M is molecular weight, and R_p (nm) is particle radius.

In the next section, mass transfers can be modeled from two elementary steps and then related to each other as well as the particle growth.

2.1.1. Adsorption/Desorption Process. The adsorption/desorption of ions are governed by the adsorbed concentration, bulk concentration, and available space within the surfactant layer. Following the adsorption/desorption principle,[17] the adsorption is proportional to the bulk concentration and vacant space. However, the desorption is proportional to the adsorbed concentration. Hence, adsorption and desorption rates per area unit are given by

$$r_{ads,i} = K_{ads,i}\Gamma_{vacant,i}c_i \quad (4)$$

$$r_{des,i} = K_{des,i}\Gamma_i \quad (5)$$

where $K_{ads,i}$ (M^{-1} s^{-1}) and $K_{des,i}$ (s^{-1}) are rates of the adsorption and desorption ($i = Fe^{3+}$ and H_3O^+), c_i (M) and Γ_i (mol/m^2) are the bulk concentration and adsorbed concentration of each species, and $\Gamma_{vacant,i}$ is the vacant sites within surfactant layer for species i.

The regulating role of surfactant layer is mathematically quantified though the "penetrability" of surfactant zone. The penetrability is defined by the available area of the ion penetration and denoted as $S_{e,m}$ (as a percentage of total surface area). The value of $S_{e,m}$ should be small (~10%) and controlled by the surfactant structure. By reducing $S_{e,m}$, the surfactant layer

DOI: 10.1021/acs.jpca.7b02186
J. Phys. Chem. A 2017, 121, 3213−3219

can reduce the available space for ions adsorption. The theoretical (maximum) vacant sites for each ion are given by

$$\Gamma_{m,i} = \frac{10^{18}}{N_a}\frac{S_{e,m}}{A_{a,i}} \tag{6}$$

where $\Gamma_{m,i}$ (mol/m^2) and $A_{a,i}$ are maximum space within surfactant layer and specific ionic area (nm^2) for ion i, and N_a is Avogadro number.

It should be noted that, for the same value of $S_{e,m}$, $\Gamma_{m,i}$ can be different for different ions. Larger ion, such as Fe^{3+}, has smaller $\Gamma_{m,i}$. During the particle growth, some of the available space is occupied by the adsorbed Fe^{3+} and H_3O^+ (as represented by Γ_{Fe} and Γ_{H3O}). Hence, the actual available space is reduced by these ions and is given by

$$S_{e,a} = S_{e,m} - \frac{N_a}{10^{18}}(A_{a,Fe}\Gamma_{Fe} + A_{a,H3O}\Gamma_{H3O}) \tag{7}$$

Hence, the vacant spaces for each ions are reduced correspondingly. The vacant space within surfactant zone for each specie equal to $S_{e,a}$ divided by specific area of each ion:

$$\Gamma_{vacant,Fe} = \frac{10^{18}S_{e,m}}{N_a A_{a,Fe}} - \left(\Gamma_{Fe} + \frac{A_{a,H3O}}{A_{a,Fe}}\Gamma_{H3O}\right) \tag{8}$$

$$\Gamma_{vacant,H_3O} = \frac{10^{18}S_{e,m}}{N_a A_{a,H3O}} - \left(\frac{A_{a,Fe}}{A_{a,H3O}}\Gamma_{Fe} + \Gamma_{H3O}\right) \tag{9}$$

Consequently, the net mass transfer (mol/s) due to adsorption/desorption between the bulk to surfactant layer is given:

$$Q_{a,Fe} = A_p\{K_{ads,Fe}\Gamma_{vacant,Fe}c_{Fe} - K_{des,Fe}\Gamma_{Fe}\} \tag{10}$$

$$Q_{a,H3O} = A_p\{K_{ads,H3O}\Gamma_{vacant,H3O}c_{H3O} - K_{des,H3O}\Gamma_{H3O}\} \tag{11}$$

where Q_a is the mass transfers and A_p (nm^2) is the surface area of particle (which equals $4\pi R_p^2$).

It should be noted that Q_a can be either positive or negative, depending on the concentrations.

2.1.2. Binding/Dissolution Process. The binding of the Fe^{3+} to the solid surface is proportional to Fe^{3+} concentration in surfactant layer.[19] The dissolution reaction depends on H_3O^+ concentration. The binding and dissolution reactions of solutes into solid surface are given by

$$r_{bind} = K_{binding}A_p\Gamma_{Fe} \tag{12}$$

$$r_{diss} = K_{diss}A_p\Gamma_{H_3O}^3 \tag{13}$$

where $r_{binding}$ and r_{diss} (mol/s) are the rates of forward and backward reaction, $K_{binding}$ (1/mol s) and K_{diss} (1/mol^2 m^4 s) are binding and dissolution constants.[17,20]

The net rate of the reaction (forming FeOOH in mol/s) is given by

$$Q_r = r_{bind} - r_{diss} = A_p[K_{binding}\Gamma_{Fe} - K_{diss}\Gamma_{H_3O}^3] \tag{14}$$

The changes of each species in surfactant layer are governed by both adsorption/desorption (eqs 10 and 11) and chemical reaction (eq 14):

$$\frac{d\Gamma_{Fe}}{dt} = \{K_{ads,Fe}\Gamma_{vacant,Fe}c_{Fe} - K_{des,Fe}\Gamma_{Fe}\} - [K_{binding}\Gamma_{Fe} - K_{diss}\Gamma_{H_3O}^3] \tag{15}$$

$$\frac{d\Gamma_{H3O}}{dt} = \{K_{ads,H3O}\Gamma_{vacant,H3O}c_{H3O} - K_{des,H3O}\Gamma_{H3O}\} + 3[K_{binding}\Gamma_{Fe} - K_{diss}\Gamma_{H_3O}^3] \tag{16}$$

The system of two ODEs, eqs 15 and 16, can be solved numerically for any given initial values. The initial values for adsorbed concentrations can be assumed:

$$\Gamma_{H3O,t=0} = \Gamma_{Fe,t=0} = 0 \tag{17}$$

Since the process is reaction controlled, it can be assumed that c_i are constant throughout the process. It should be noted that the dissolution constant would be very low in comparison with the binding reaction. Hence, the dissolution reaction can be ignored ($K_{diss} = 0$). Once the transient adsorption/reaction rate are solved, the particle size can be calculated by eqs 3 and 14:

$$\frac{dR_p}{dt} = \frac{M}{\rho}[K_{binding}\Gamma_{Fe} - K_{diss}\Gamma_{H_3O}^3] \tag{18}$$

Equation 18 requires an initial value of particles, which is the nuclei size:

$$R_{p,t=0} = R_n \tag{19}$$

where R_n is the nuclei size.

The above system has a number of physical parameters and process-related parameters. The physical parameters (Table 1)

Table 1. Physical Constants

parameters	value	justification
c_{Fe3+}	0.002 M	solubility
c_{H3O+}	0.1 M	pH
A_{Fe}	0.0346	from iron diameter of 0.275 nm[21]
A_{H3O}	0.0594 nm^2	from hydronium diameter of 0.21 nm[21]
ρ_{FeOOH}	3 kg/L	density[22]
ρ_{Fe3O2}	5.24 kg/L	density

are defined from experimental values. The processes related include the four adsorption and two kinetic constants, as well as R_n and $S_{e,m}$. These parameters are difficult to verify. However, the only surfactant-controlled parameters are R_n and $S_{e,m}$. The other variables (Table 2) are independent of surfactants. If surfactant is changed, while the reagents/reactions are maintained in the same conditions, then only $S_{e,m}$ and R_n are variable. The value of R_n should remain around 0.1 and 0.3 nm and has an insignificant effect on particle size as shown later. Hence, $S_{e,m}$ is the key parameter of the model.

Table 2. Adsorption/Reaction Parameters

parameters	value
$K_{ads,H3O}$	0.25 s^{-1} M^{-1}
$K_{ads,Fe}$	2.5 s^{-1} M^{-1}
$K_{des,H3O}$	100 s^{-1}
$K_{des,Fe}$	100 s^{-1}
$K_{binding}$	2 s^{-1}
K_{diss}	0

DOI: 10.1021/acs.jpca.7b02186
J. Phys. Chem. A 2017, 121, 3213−3219

To demonstrate the role of $S_{e,m}$ on the process, two values (11% and 5%) were used. It can be seen in Figure 2 that the

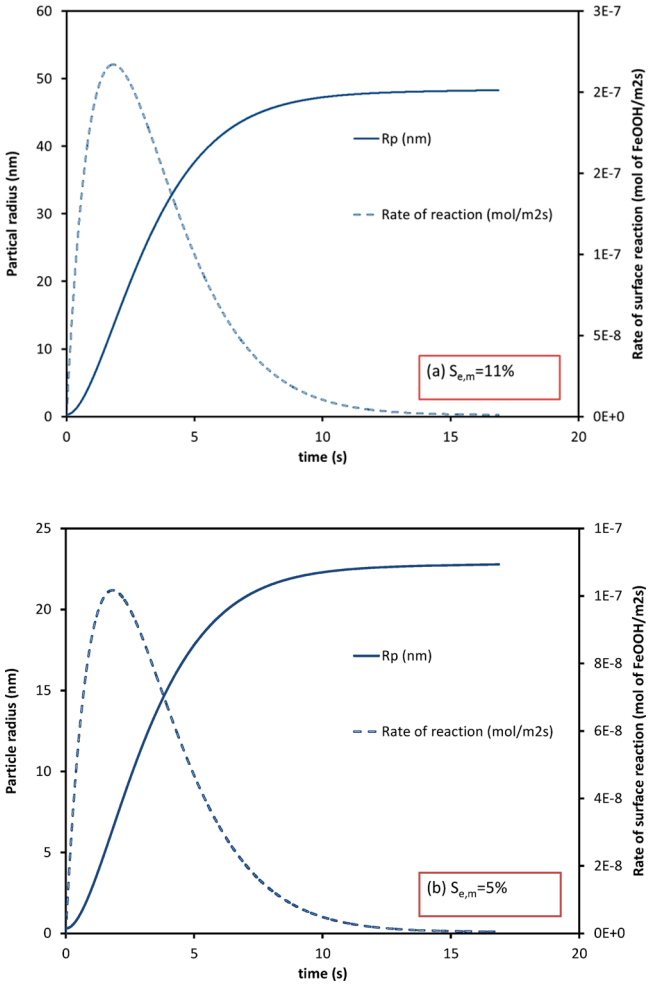

Figure 2. Particle growth as a function of time, with $S_{e,m}$ of (a) 11% and (b) 5% (other parameters are tabulated in Table 2.).

growth of particles was significantly altered by the value of $S_{e,m}$. The particle radius reached a plateau within 20 s, yet the value was almost halved from 49 to 26 nm. The smaller $S_{e,m}$ reduced the reaction rate and particle size correspondingly. It should be noted that there could be many combinations of parameters in Table 2 to produce similar results. However, the correlation between $S_{e,m}$ and particle size remains the same. The radius at 20 s will be taken as final particle size. The value of R_n is assumed at 0.3 nm, which is the micelle size.[9] From the model, eq 19 and Figure 2, it can be seen that R_n has an insignificant effect on the final particle size.

2.2. Surfactant and Penetrability. In this section, the value of $S_{e,m}$ is related to surfactant structure. As evidenced in the literature, the binding of ions to particle surface should be regulated by the surfactant length.[1] Hence, one would expect $S_{e,m}$ is variable with surfactant molecules, $C_nH_{2n+2}(CH_3)_3NBr$. In the other words, there should be a strong correlation between n and $S_{e,m}$. In order to quantify the $S_{e,m}$ versus n relationship, we need establish the relationship between n and the surfactant adsorption.

Since the surfactant does not involve with reaction, the layer remains unchanged during the particle growth. The adsorption of surfactant is in equilibrium with monomer concentration in the bulk. The adsorbed surfactant is given by the well-known Langmuir adsorption isotherm:

$$\frac{\Gamma_{surf}}{\Gamma_m} = \frac{K_s c_{surf,1}}{1 + K_s c_{surf,1}} \tag{20}$$

where $c_{suf,1}$ is concentration of surfactant monomer in the bulk, K_s (M^{-1}) is the equilibrium constant for adsorption process, and Γ_{surf} and Γ_m are adsorbed and maximum adsorption (mol/m^2), respectively.

It should be noted that $c_{suf,1}$ is the surfactant monomer, not the total surfactant concentration. Above the critical micelle concentration (CMC), surfactants can exist in monomer and micelles. If surfactant concentration is higher than CMC, $c_{suf,1}$ is capped at c_{CMC}, while all excessive surfactant molecules are in micelles. The equilibrium between monomer and micelles are governed by well-known thermodynamic equilibrium.[23] Most experiments employ surfactants at above CMC concentration (to maintain a constant adsorption layer). At above CMC concentrations, the shape and aggregation number of micelles have no influence on the adsorption layer. The saturated adsorption layer is given by

$$\Gamma_{surf} = \Gamma_m \frac{K_s c_{cmc}}{1 + K_s c_{cmc}} \tag{21}$$

On the iron oxide surface, the surfactant adsorption is governed by interaction with ionic heads. For this system, one can assume that K_s and Γ_m are the same for all surfactants. The value of Γ_m should be directly estimated from the size of tetramethylammonium bromide, $\sim 6.2 \times 10^{-6}$ mol/m^2.[24] In order to quantify the relationship between n and Γ_{surf}, one needs to correlate c_{CMC} to n. Fortunately, such relationship has been well-established for single branch surfactants: log c_{cmc} increases linearly with increasing carbon number.[25] The linear relationship is given as

$$\log c_{cmc} = A + Bn \tag{22}$$

where A and B are mathematical constants.

The above equation is universally applicable to all anionic and cationic surfactants.[25] With the reported CMC of alkyl trimethylammonium,[26,27] the values of A and B can reliably obtained for these surfactants (as shown in Table 3).

Table 3. Surfactant Parameters

	value	justification
A	−3.68	from CMC data and eq 22
B	−0.185	from CMC data and eq 22
Γ_m (mol/m^2)	6.2×10^{-6} mol/m^2	from the size of $(CH3)_4N^{+}$[24]
K (M^{-1})	250	adsorption constant

Equations 20 and 21 can quantify the relationship between n (surfactant length) and Γ_{surf}, as shown in Figure 3.

Finally, one needs to establish the relationship between Γ_{surf} and $S_{e,m}$. In our model, we assume that the vicinity of surfactant head is penetrable by ions. The underlining reason is that the ionic head is relatively large with non-neutral charge distribution (between nitrogen and three methyl groups). The charged layer is in an equilibrium with ions in the bulk.[28] Hence, $S_{e,m}$ is directly proportional to number of surfactant heads on the surfactant layer. In the other words, $S_{e,m}$ is proportional to Γ_{surf} and given by

DOI: 10.1021/acs.jpca.7b02186
J. Phys. Chem. A 2017, 121, 3213−3219

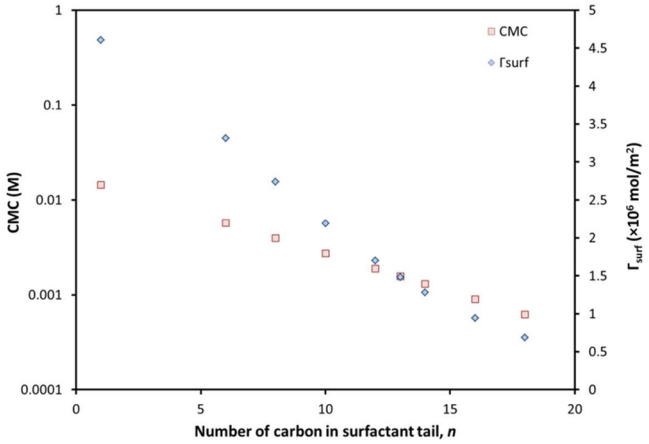

Figure 3. CMC and surfactant adsorption for C_nTAB. CMC is calculated from eq 22. Γ_{surf} is calculated from eq 21.

$$S_{e,m} = \beta \frac{N_a}{10^{18}} \Gamma_{surf} A_{surf} \tag{23}$$

where β is positive and small constant (<1) and A_{suf} is surface area of surfactant head (nm^2).

With these equations, eqs 20−23, one can directly quantify $S_{e,m}$ as a function of n. Consequently, the numerical model can predict the particle size as a function of carbon length.

3. EXPERIMENTAL SECTION

3.1. Materials. To verify the theory, the Fe_2O_3 thin films were prepared with different surfactants via sol−gel method on solid substrates. Eight cationic surfactants with increasing carbon number were employed (as listed in Table 4). The

Table 4. Chemicals

name	formula	grade (%)
iron(III) nitrate	$Fe(NO_3)_3{\cdot}9H_2O$	99.9
1-butyl-1-methylpyrrolidinium bromide	$C_9H_{20}BrN$	99
octyltrimethyllammonium bromide	$C_{11}H_{26}BrN$	99
decyltrimethylammonium bromide	$C_{13}H_{30}BrN$	99
dodecyltrimethylammonium bromide	$C_{15}H_{34}BrN$	99
tetrabutylammonium bromide	$C_{16}H_{36}BrN$	99
tetradecyltrimethylammonium bromide	$C_{17}H_{38}BrN$	99
cetyltrimethylammonium bromide	$C_{19}H_{42}BrN$	99
octadecyltrimethylammonium bromide	$C_{21}H_{46}BrN$	99

general formula of the surfactants is $C_nH_{2n+2}(CH_3)_3NBr$, with n = 6, 8, 10, 12, 13, 14, 16, and 18. It is essential that the procedure and precursors are employed in the same conditions. Hence only variable factor in the experiment is the surfactant length. All chemicals were obtained from Sigma-Aldrich. It should be noted that $C_6H_{14}(CH_3)_3NBr$ and $C_{13}H_{28}(CH_3)_3NBr$ are not straight carbon-chain surfactants. They were commercially available and thus included to fulfill the data.

3.2. Preparation of the Precursor Solutions. The Fe_2O_3 thin films were prepared via sol−gel spin coating method onto FTO glass slides. Eight FTO glasses had been subsequently rinsed in ultrasonic bath with deionized water, ethanol, and acetone before they were dried by nitrogen gas for 10 min. For each sample, 0.5 g of each surfactant was added to 4 mL of deionized water. The concentrations of all surfactants were above the CMC and thus warrant the model requirements. These solutions were stirred for 30 min, before adding 2 g of iron(III) nitrate, and then stirring for 2 h. Sol−gel spin coating method was used to subsequently deposit the samples as the following steps: (1) Drop prepared solution onto FTO substrate that tightly held on the chuck of spin coater, (2) two fixed speeds (50 rpm, 100 rpm) that used to rotate the substrate for 1 min in total, and (3) each sample was heated on a ceramic plate at 60 °C for 30 min before placing in the furnace at 450 ± 1 °C, for 4 h, in air, with fixed heating and cooling rate of 5 °C/min.

3.3. Characterization of the Films. A combination of complementary analytical techniques was employed to quantify the differences of the prepared samples. The structure of the thin films were verified by using Field emission scanning electron microscopy (FE-SEM MIRA3, Tescan). However, the particle size was determined by X-ray diffraction (XRD, Bruker D8 Advance) with Cu Kα radiation (λ = 0.15418 nm) and for qualitative analysis, XRD diagrams were recorded in the interval $20° \leq 2\theta \leq 70°$ at scan rate of 0.01 °/s. These characterization results exhibited insights into the structures of the samples and explained the effects of different tail lengths on nanoparticle size.

4. RESULT AND DISCUSSION

4.1. Surface Morphology. The morphology of the films was investigated by field emission scanning electron microscopy (FESEM) operating at 3 kV for the top size of the films. The SEM micrographs presented qualitatively the effects of surfactant tails on the size of Fe_2O_3 nanoparticle. The largest particle size was obtained with smallest surfactant. Examples can be seen in Figure 4. The quantitative size analysis is based on XRD.

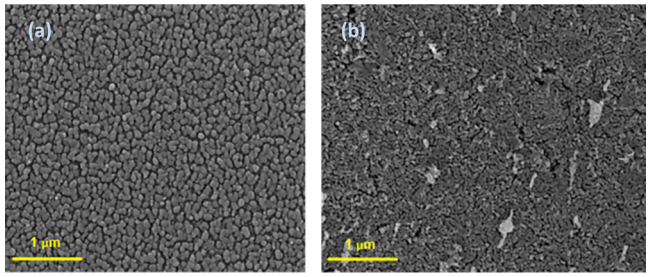

Figure 4. SEM images of cationic surfactants treated Fe_2O_3 nanoparticles (a) $C_{13}H_{30}BrN$ and (b) $C_{21}H_{46}BrN$.

Crystalline properties and the phase formation were investigated by X-ray diffraction analysis (Figure 5). The Fe_2O_3 peaks were observed at 2θ an are, respectively 28.09°, 38.65°, 42.44°, 47.86°, 58.08°, 64.72°, 67.65°, 74.84°, and 76.85°. It is worth noting that no any surfactant-corresponded peak was observed, which proved a completed removal of the surfactants after the calcination.

4.2. Particle Size. The average crystallite size of Fe_2O_3 from XRD was calculated from the Debye−Scherrer equation.[11] The data showed a gradual decrease with increasing surfactant length (Figure 6). The largest particle size was obtained with smallest surfactant, while the Fe_2O_3 nanoparticles with their average size only 25 nm were accounted by the longest (n = 18) surfactant.

The behavior was consistent with previous data.[1] It is well-known that micelle size increases with increasing surfactant length.[9,13] Hence, the nuclei size, which is proportional to

DOI: 10.1021/acs.jpca.7b02186
J. Phys. Chem. A 2017, 121, 3213−3219

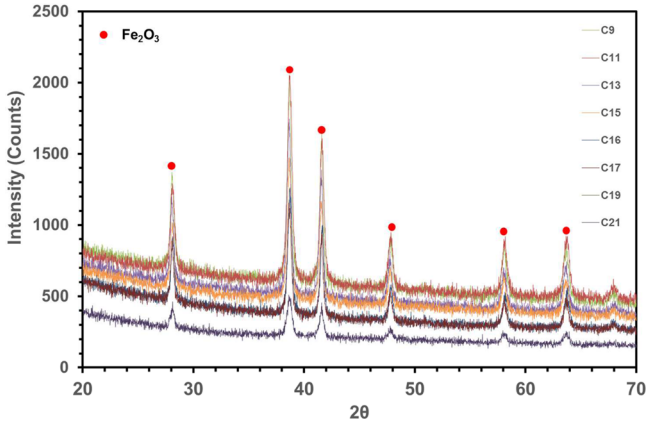

Figure 5. X-ray diffraction patterns for annealed samples of Fe_2O_3 with different surfactants.

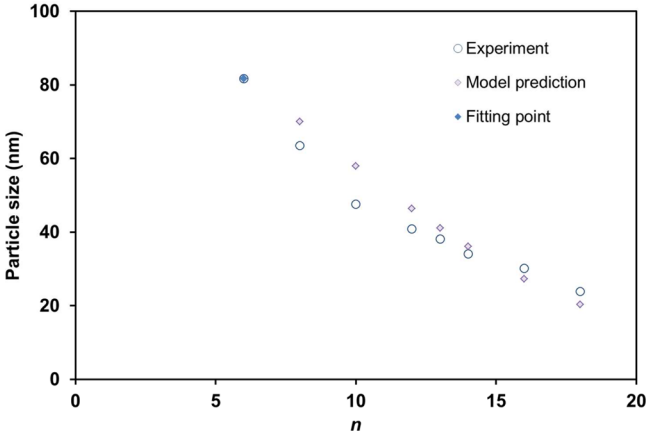

Figure 6. Particle size as a function of the surfactant length (β = 25%). The model was fitted at n = 6 and used to predict particle size with other surfactants.

micelle size, cannot be used to quantify the decreasing trend of particle size.

4.3. Modeling. The modeling would involve three different types of parameters: the constants for chemical reactants (in Tables 1 and 2), the surfactant's parameters (in Table 3), the nuclei size (R_n), and β. As mentioned above, the constants in Tables 1−3 are independent of surfactants. The value of β is obviously independent of surfactant tails. While the value of R_n should be varied with surfactant length, the variation in R_n should be in the same order of micelle size and remain within 0.2 to 0.3 nm. Consequently, an increment in R_n (from C_6 to C_{18}TAB) may increase the final particle size by 0.1 nm, as shown in the modeling. Such increment is negligible for the particle range in Figure 4.

In summary, all parameters (excepting R_n) are independent of the surfactant length. The variation of R_n should remain within ~0.1 nm and hence has a negligible effect on the final particle size. With constants fixed in Tables 1−3, the only fitting parameter is β. In this case, the value of β was varied to match the particle size synthesized from C_6TAB. The required β was obtained at 25%. Subsequently, the particle sizes were reproduced for the other surfactants, without further fitting.

It can be seen that the model predicts the particle size very well. The successful prediction validates the theoretical model. The correlation between surfactant size and particle size was confirmed both experimentally and theoretically. This is the first time that the particle growth is predicted from the reaction-limited process. The framework can be extended to other metal and surfactant systems in wet synthesis. For WO_3,[11] it has been found that the particle size also decreased with increasing size of surfactants. However, the surfactants in that case were nonionic surfactants and thus different equations are needed to replaced (eqs 20−22). A proper understanding of the surfactant-controlled kinetics would be very helpful to selective surfactants for directional particle growth.[7] For instance, the correlation between surfactant size and growth rate can be used in binary surfactant systems[29] and control the shape factor of nonspherical particles. The nature of ion "penetrability" in surfactant layer can be explored further though molecular simulations,[27] and lead to other applications of surfactant.

5. CONCLUSION

The study developed a theory on the correlation between nanoparticle size and the characteristics of capping agent. Specifically, the role of capping agents (surfactants) was quantified by solving adsorption/desorption and reactions steps. The model relates the surfactant size and particle size through a single parameter: the ion "penetrability" in surfactant layer. The theory correctly predicts the experimental results for iron oxide and cationic surfactants.

There are a number of important conclusions. First, the nuclei size, which is proportional to micelle size, was not a decisive factor in determining final particle size. Second, both reaction and adsorption/desorption steps play crucial roles in determining particle size. Third, the theoretical and experimental results provide the first quantitative insight into the role of the surfactant length on nanoparticle formation.

The model provides a simple pathway to precisely control the particle size. The modeling is applicable to other metal oxides, such as TiO_2, ZnO, and WO_3, with appropriate reaction and adsorption coefficient.

AUTHOR INFORMATION

Corresponding Author

*E-mail: c.phan@curtin.edu.au.

ORCID

Chi M. Phan: 0000-0002-1565-8193

Notes

The authors declare no competing financial interest.

REFERENCES

(1) Memar, A.; Phan, C. M.; Tade, M. O. Influence of surfactants on fe2o3 nanostructure photoanode. *Int. J. Hydrogen Energy* **2012**, *37*, 16835−16843.

(2) Pileni, M. P. Nanosized particles made in colloidal assemblies. *Langmuir* **1997**, *13*, 3266−3276.

(3) de Dios, M.; Barroso, F.; Tojo, C.; López-Quintela, M. A. Simulation of the kinetics of nanoparticle formation in microemulsions. *J. Colloid Interface Sci.* **2009**, *333*, 741.

(4) Scorciapino, M. A.; Sanna, R.; Ardu, A.; Orrù, F.; Casu, M.; Musinu, A.; Cannas, C. Core-shell nano-architectures: The incorporation mechanism of hydrophobic nanoparticles into the aqueous core of a microemulsion. *J. Colloid Interface Sci.* **2013**, *407*, 67.

(5) Jun, Y.-w.; Choi, J.-s.; Cheon, J. Shape control of semiconductor and metal oxide nanocrystals through nonhydrolytic colloidal routes. *Angew. Chem., Int. Ed.* **2006**, *45*, 3414−3439.

(6) Nguyen, T.-D. From formation mechanisms to synthetic methods toward shape-controlled oxide nanoparticles. *Nanoscale* **2013**, *5*, 9455.

DOI: 10.1021/acs.jpca.7b02186
J. Phys. Chem. A 2017, 121, 3213−3219

(7) Yin, Y.; Alivisatos, A. P. Colloidal nanocrystal synthesis and the organic-inorganic interface. *Nature* **2005**, *437*, 664−670.
(8) Pinazo, A.; Pérez, L.; Lozano, M.; Angelet, M.; Infante, M. R.; Vinardell, M. P.; Pons, R. Aggregation properties of diacyl lysine surfactant compounds: Hydrophobic chain length and counterion effect. *J. Phys. Chem. B* **2008**, *112*, 8578.
(9) Oliver, R. C.; Lipfert, J.; Fox, D. A.; Lo, R. H.; Doniach, S.; Columbus, L. Dependence of micelle size and shape on detergent alkyl chain length and head group. *PLoS One* **2013**, *8*, e62488.
(10) Pileni, M. P. The role of soft colloidal templates in controlling the size and shape of inorganic nanocrystals. *Nat. Mater.* **2003**, *2*, 145−150.
(11) Memar, A.; Phan, C. M.; Tade, M. O. Controlling particle size and photoelectrochemical properties of nanostructured wo_3 with surfactants. *Appl. Surf. Sci.* **2014**, *305*, 760−767.
(12) Erdemir, D.; Lee, A. Y.; Myerson, A. S. Nucleation of crystals from solution: Classical and two-step models. *Acc. Chem. Res.* **2009**, *42*, 621−629.
(13) Tanford, C. Micelle shape and size. *J. Phys. Chem.* **1972**, *76*, 3020−3024.
(14) Bhimaraj, P.; Yang, H.; Siegel, R. W.; Schadler, L. S. Crystal nucleation and growth in poly(ethylene terephthalate)/alumina-nanoparticle composites. *J. Appl. Polym. Sci.* **2007**, *106*, 4233−4240.
(15) Leubner, I. H. Crystal formation (nucleation) under kinetically-controlled and diffusion-controlled growth conditions. *J. Phys. Chem.* **1987**, *91*, 6069−6073.
(16) LaMer, V. K.; Dinegar, R. H. Theory, production and mechanism of formation of monodispersed hydrosols. *J. Am. Chem. Soc.* **1950**, *72*, 4847−4854.
(17) Rempel, J. Y.; Bawendi, M. G.; Jensen, K. F. Insights into the kinetics of semiconductor nanocrystal nucleation and growth. *J. Am. Chem. Soc.* **2009**, *131*, 4479−4489.
(18) Flynn, C. M. Hydrolysis of inorganic iron(iii) salts. *Chem. Rev.* **1984**, *84*, 31−41.
(19) Yates, D. E.; Levine, S.; Healy, T. W. Site-binding model of the electrical double layer at the oxide/water interface. *J. Chem. Soc., Faraday Trans. 1* **1974**, *70*, 1807−1818.
(20) Kalinin, V. V.; Radke, C. J. An ion-binding model for ionic surfactant adsorption at aqueous-fluid interfaces. *Colloids Surf., A* **1996**, *114*, 337−350.
(21) Marcus, Y. Ionic radii in aqueous solutions. *Chem. Rev.* **1988**, *88*, 1475−1498.
(22) Maeda, H.; Maeda, Y. Measurement of density distributions for colloidal β-feooh rods in suspensions exhibiting phase separation: The role of long-range forces in smectic ordering. *J. Chem. Phys.* **2004**, *121*, 12655−12665.
(23) Israelachvili, J. N. *Intermolecular and Surface Forces*, 3rd ed.; Academic Press, 2011.
(24) Gilányi, T.; Varga, I.; Stubenrauch, C.; Mészáros, R. Adsorption of alkyl trimethylammonium bromides at the air/water interface. *J. Colloid Interface Sci.* **2008**, *317*, 395−401.
(25) Rosen, M. J.; Kunjappu, J. T. *Surfactants and Interfacial Phenomena*, 4th ed.; Wiley: Hoboken, 2012.
(26) Bergeron, V. Disjoining pressures and film stability of alkyltrimethylammonium bromide foam films. *Langmuir* **1997**, *13*, 3474−3482.
(27) Phan, C. M.; Le, T. N.; Nguyen, C. V.; Yusa, S.-i. Modeling adsorption of cationic surfactants at air/water interface without using the gibbs equation. *Langmuir* **2013**, *29*, 4743−4749.
(28) Phan, C. M. Dissociation of ionic surfactants at the air/water interface: Complete or partial? *J. Phys. Chem. B* **2016**, *120*, 7681−7686.
(29) Jun, Y.-w.; Casula, M. F.; Sim, J.-H.; Kim, S. Y.; Cheon, J.; Alivisatos, A. P. Surfactant-assisted elimination of a high energy facet as a means of controlling the shapes of tio2 nanocrystals. *J. Am. Chem. Soc.* **2003**, *125*, 15981−15985.

DOI: 10.1021/acs.jpca.7b02186
J. Phys. Chem. A 2017, 121, 3213−3219